Initial determination of the spins of the gluino and squarks at LHC

Gordon L Kane[1]**, Alexey A Petrov**[1,2]**, Jing Shao**[1] **and Lian-Tao Wang**[3]

[1] Michigan Center for Theoretical Physics, University of Michigan, Ann Arbor, MI 48109, USA
[2] Department of Physics and Astronomy, Wayne State University, Detroit, MI 48201, USA
[3] Physics Department, Princeton University, Princeton, NJ 08544, USA

Abstract

In principle particle spins can be measured from their production cross sections once their mass is approximately known. The method works in practice because spins are quantized and cross sections depend strongly on spins. It can be used to determine, for example, the spin of the top quark. Direct application of this method to supersymmetric theories will have to overcome the challenge of measuring mass at the Large Hadron Collider, which could require high statistics. In this paper, we propose a method of measuring the spins of the colored superpartners by combining rate information for several channels and a set of kinematical variables, without directly measuring their masses. We argue that such a method could lead to an early determination of the spin of gluino and squarks. This method can be applied to the measurement of spin of other new physics particles and more general scenarios.

(Some figures in this article are in colour only in the electronic version)

1. Introduction

The upcoming experiments at the Large Hadron Collider (LHC) will shed light on the solutions of the shortcomings of the Standard Model (SM), and should identify new degrees of freedom associated with the new physics. Most of the leading candidates for such physics involve supersymmetry, which predicts doubling of the observed particle spectrum. It is expected that some of the supersymmetric partners of the SM particles will be produced at the LHC. It will be essential to confirm that the candidate superpartners indeed differ by half a unit in spin from their partners in order to be confident that it is indeed supersymmetry that is being discovered. A rigorous determination of the spins of new particles will be difficult and complicated, particularly early with limited statistics, and will require a detailed analysis of decay angular distributions and correlations [1–7]. Though it will be necessary to do this eventually, we want to argue that an initial determination of the spins can be made in many cases, particularly for particles that dominate production. If the new physics is indeed supersymmetric, the initial

production of colored superpartners is likely (though not certain) to dominate, and we focus on a preliminary measurement of their spins. As an illustration of the method, we apply it to the determination of the spin of the top quark, whose measurement by this approach does not seem to have been previously reported. The top-quark analysis illustrates both the strength and limitations of the method, clearly distinguishing a spin-1/2 'top quark' from a spin-0 one, but not from a spin-1 one.

A standard way of testing a theory, such as supersymmetry, is by comparing theoretical predictions with experimental data. Given preliminary observation of a signal for a new particle, the minimal test would simply involve calculation of the production rate for a particle of a given spin, color and other quantum numbers, and checking that the theory and data are consistent. For instance, the production rates of colored superpartners, like that of the top quarks, are largely determined by their QCD interactions, so these checks do not depend significantly on other features of the chosen model of physics beyond the SM.

Such a test can only be performed once the particle's mass is measured, since the production rate depends on the mass. In order to test a particular model, one can in addition compare the production rates computed within this model with that of some alternative scenario—comparisons are normally less sensitive to systematic uncertainties such as cross-section normalization errors. For example, for the top quark, one can compute the rate for the particle in the same representation of color group, but of different spin, say zero or one. These rates would differ significantly both because of the number of spin degrees of freedom and because of different angular momentum configuration of the final state; depending on their spin, the final state particles can be produced in either *s*- or *p*-wave. As it turns out, the latter effect is significant even at a hadron collider. As we shall see, even an approximate measurement of the mass provides good discrimination between the cases of different spin, simply because the resulting production rates are very different. This implies that one can determine the spin of the produced particles even with the limited-luminosity early measurements of production cross sections and mass. The results can of course be improved with more data and analysis. Similarly, we will compare alternative spin scenarios for color octet 'gluinos'. The method can later be extended to test both the color and spin separately.

Of course accurate calculations of cross sections of strongly interacting particles require inclusion of higher order QCD effects. In order to demonstrate the effectiveness of the method, here we only consider the rates computed at the tree level. Indeed, the choice of the renormalization and factorization scales, as well as other effects, will bring additional uncertainty into evaluation of the absolute rates. For a given mass, the effects of such uncertainties will be essentially the same for the different spin cases. However, as we shall show in this paper, the relevant comparison is between different spin scenarios with *different* mass scales. Therefore, the effect of higher order QCD corrections do not cancel in this comparison. Nevertheless, we shall argue that such corrections will not change the rate in ways that significantly affect the effectiveness of our method.

It can be challenging to measure the mass of a particle, particularly at a hadron collider. Most importantly, typical kinematical variables, such as H_T or m_{eff}, essentially measure the *mass differences* between the produced particle and its decay chain members. Absolute mass scale can seldom be determined from these variables in scenarios such as supersymmetry, where the end product of a decay chain is a massive neutral stable particle which escapes detection. With only information about rates in certain channels and mass differences, as we will discuss in detail below, there are typically degeneracies between supersymmetry and other scenarios with different spin partners.

Studies of mass determination using detailed kinematical information were performed in [8–21]. Application of these methods typically requires rather high statistics. Moreover, such

mass measurement would have to be fairly accurate in order to be useful for spin determination. Since the rate scales with a high power of mass, a small error in mass measurement could translate into a large uncertainty in rate predictions. In this paper, we suggest a rather different method. Instead of trying to measure the mass directly, we propose to combine the rate of several channels and a set of commonly used kinematical distributions. We demonstrate that this method allows us to break the degeneracy and could lead to an early determination of the spins of the new particles produced at the LHC.

Ideally, one would also like to measure gauge couplings, color charges and electroweak charges of the new particles, which are also predicted by the theory, and also test spins of other particles (e.g. charginos and neutralinos) that are produced with smaller rates and/or in decay chains. Such rates and branching ratios do depend on particle spins, so once the spins and masses of the particles that are dominantly produced are determined, some tests or determinations of others may be possible, depending on how well the relevant signals can be isolated. Some constraints on color charges can be checked fairly simply. For example, if gluinos are produced from color octet gluons, their color representation can be $8 \otimes 8 = 1 + 8 + 8 + 10 + \overline{10} + 27$, and one can calculate the production cross sections holding other quantum numbers fixed. It is appropriate to proceed by initially checking one property at a time (such as spin), setting others (such as color) at their expected values. As more statistics become available, several variables can be simultaneously varied.

This paper is organized as follows: we motivate our discussion by considering measurement of the top-quark spin in section 2, provide basic set-up in section 3 and apply the proposed method to determination of the spin of gluino in section 4. We conclude in section 5.

2. Motivation: determining the spin of the top quark

In this section, we briefly discuss the method of determining the spin of a candidate top quark, denoted 'top quark', with production rate information. The production of the top quark at the Tevatron is dominated by the s-channel process $q\bar{q} \to t\bar{t}$, which implies that the cross section is proportional to the velocity β of the produced top quark near the kinematical threshold. However, if instead scalar particles are produced, the configuration of the final state must be CP even and so the cross section is dominantly p-wave and is proportional to β^3 near the threshold. Thus, we expect the spin-1/2 'top quark' to have a larger production rate than spin-0. In figure 1, we plot the cross sections as functions of mass of the 'top quark', where we also included the gluon fusion process. The production cross-section for spin-0 'top quarks' is indeed significantly below that for the spin-1/2 'top quark'. Thus given the mass of the 'top quark', the magnitude of the production cross-section strongly favors the case of spin-1/2 'top quark'[4].

3. Cross section for colored partners with different spin

In this section, we compare the production cross-sections of colored superpartners and their counterparts (with different spin) in alternative scenarios.

For the purpose of illustrating the idea, we implemented a simple same-spin scenario[5] where for each SM quark q there is a massive same-spin partner q' and for the SM gluon there

---

[4] Indeed, it should be remarked that if a top-quark candidate decays into a SM b-quark and a W boson, it can only have a half-integral spin.

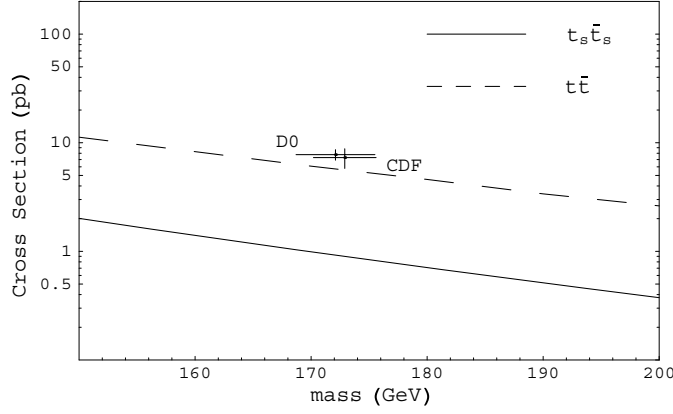[5] One should note that this is not the case of the Universal Extra-Dimension (UED) scenario [27].

Figure 1. Cross section as a function of the 'top quark' mass at the Tevatron. The lower dashed line is for the case of spin1/2 'top quark', and the solid line is for the case of spin-0 'top quarks'. The two points with error bars show the CDF and D0 data for the top mass and cross section with one σ error [22–25].

is a same-spin partner g'. Results for models with more extended fermion partner sectors could be obtained by scaling from our result. The coupling relevant for production is schematically,

$$\mathcal{L}_{\text{int}} = \bar{q}'_L g' q_L + \bar{u}'_R g' u_R + \bar{d}'_R g' d_R \tag{1}$$

We begin with spin-0, spin-1/2 and spin-1 color octets, denoted by (g_S)[6], $(\tilde{g})$ and (g'), respectively. The QCD interactions of these color octets with the quarks and gluon are completely fixed by gauge invariance. The parton cross sections for pair production of these particles are already calculated in [2, 33–36]. For example, at the LHC, gluon–gluon fusion leads to the following elementary cross-sections [2, 33–36]:

$$\hat{\sigma}_{gg \to g_S g_S}(\hat{s}, m_{g_S}) = \frac{\pi \alpha_s^2}{\hat{s}} \left[\left(\frac{15}{16} + \frac{51 m_{g_S}^2}{8\hat{s}} \right) \beta + \frac{9 m_{g_S}^2}{2\hat{s}^2} \left(\hat{s} - m_{g_S}^2 \right) \log \frac{1-\beta}{1+\beta} \right], \tag{2}$$

$$\hat{\sigma}_{gg \to \tilde{g}\tilde{g}}(\hat{s}, m_{\tilde{g}}) = \frac{\pi \alpha_s^2}{\hat{s}} \left[-\left(3 + \frac{51 m_{\tilde{g}}^2}{4\hat{s}} \right) \beta + \frac{9}{4} \left(1 + \frac{4 m_{\tilde{g}}^2}{\hat{s}} - \frac{4 m_{\tilde{g}}^4}{\hat{s}^2} \right) \log \frac{1+\beta}{1-\beta} \right], \tag{3}$$

$$\hat{\sigma}_{gg \to g'g'}(\hat{s}, m_{g'}) = \frac{\pi \alpha_s^2}{\hat{s}} \left[\left(9\frac{\hat{s}}{m_{g'}^2} + \frac{117}{8} + \frac{153}{4}\frac{m_{g'}^2}{\hat{s}} \right) \beta \right.$$

$$\left. + 9 \left(1 + 3\frac{m_{g'}^2}{\hat{s}} - 3\frac{m_{g'}^4}{\hat{s}^2} \right) \log \frac{1-\beta}{1+\beta} \right] \tag{4}$$

These results are obtained including diagrams with *s*-channel gluon fusion and *t*-channel gluino exchange. For the spin-0 and spin-1 cases, there is also a four-point interaction diagram. From the above result, we see that they have the same functional dependence on β, so the argument applied for the top-quark case does not apply here. However the differences in the cross sections originate from the differences in the interaction form determined by the spin structure. As for the top-quark case, one again finds the longitudinal enhancement for the cross section of the spin-1 gluino. In figure 2, cross sections at LHC of the three cases are plotted

---

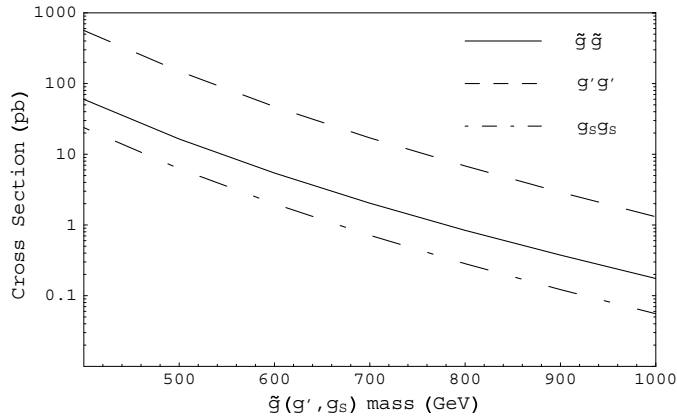[6] We consider a real scalar here.

Figure 2. A plot of the cross sections for gluino pair production (solid line), spin-1 gluon partner g' pair production (dashed line) and spin-0 gluon partner g_S pair production (dot-dashed line) at LHC. In the calculation, extra color triplets (e.g. $\tilde{q}$ or q') are taken to be 5 TeV.

as functions of the mass. In our calculation, the factorization scale μ_F and renormalization scale μ_R are set to be $\mu_F = \mu_R = m_{\tilde{g},g',g_S}$. From the plot, we can see that the cross section increases by roughly an order of magnitude as spin increases from 0 to 1 for a given mass. On the other hand, these cross sections decrease rapidly with mass. Roughly speaking, for an increase in mass by 200–300 GeV, the cross section decreases by an order of magnitude. Thus to match a given result of the cross section, the masses of gluino for different spin must be different by 200–300 GeV. This makes it possible to determine the spin by a rough mass measurement.

For later reference, we also present here the numerical results for squark pair (fermionic partner q' pair) production and squark–gluino (q'–g') associated production in figure 3. For the associated production, the cross section depends on both the squark (q') mass and the gluino (g') mass. To give a simple example and for later convenience, we choose gluino mass and g' mass such that their pair-production rate are matched. Then we plot the cross section as a functions of squark (q') mass.

The cross sections are calculated using MadGraph/MadEvent [40]. In the calculation, we use the parton distribution function CTEQ6 L [41]. The renormalization scale μ_R and the factorization scale μ_F are chosen $\mu_R = \mu_F = m_{\tilde{q},q'}$ and $\mu_R = \mu_F = 0.5 \times (m_{\tilde{q},q'} + m_{\tilde{g},g'})$ for squark (or q') pair production and squark (q')–gluino (g') associated production, respectively.

Our calculation of the parton cross sections is done at the tree level. The next-to-leading order calculation usually changes the result by a factor of order unity [30–32]. As the multiplicative K-factors always increase the production cross section, such corrections should not change the overall hierarchy of the rates for different spin assignments. The enhancement factors of the cross section for particles with different spin but in the same color representation have the same color factor and the same initial state. Although not identical, those factors are not expected to be significantly different. Note also we are not comparing cross sections at the same mass scale. As we will discuss in detail below, we will match the cross sections of particles with different spin with different masses. However, those different masses are typically within a factor of 2. Therefore, additional effects from different choices of renormalization and factorization scale will have to be included. We note that such differences in K-factors are typically quite small, about 10% [30, 32] across the mass range
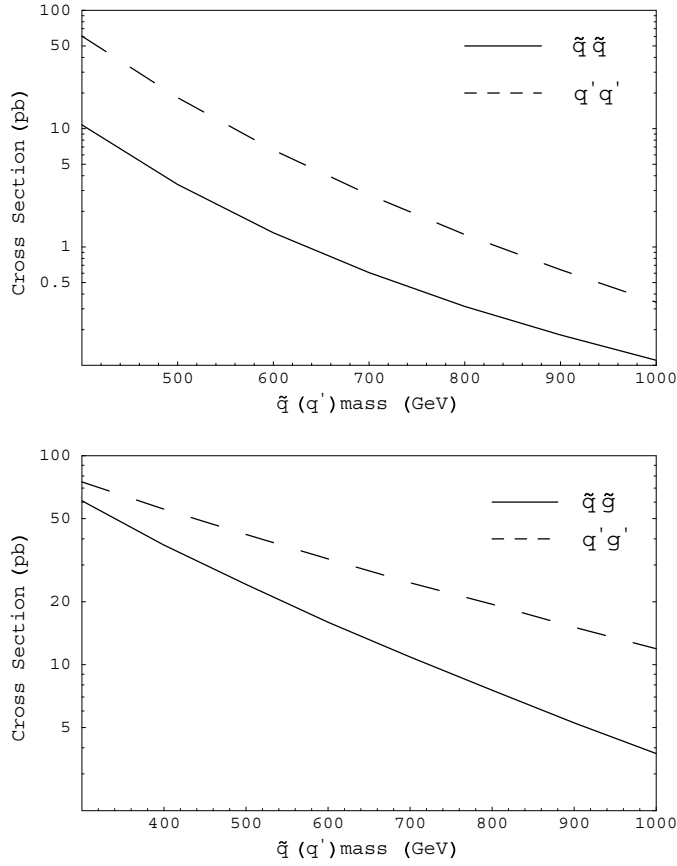
Figure 3. Top: cross sections for squark pair production (solid line) and fermionic quark partner q' pair production (dashed line) at LHC. In the calculation, gluino and g' are taken to be 5 TeV. Bottom: cross sections for squark–gluino associated production (solid line) and q'–g' associated production (dashed line) at LHC. The gluino mass and g' mass are 608 GeV and 850 GeV, respectively, in order to match the cross sections of gluino pair production and g' pair production.

we are interested in. We have also partially taken this into account by choosing μ_R and μ_F to be correlated with the masses of the particle produced.

4. Spin determination

In this section, we present our study of spin determination for the possible cases where degeneracy could occur. First, we briefly review and clarify the degeneracy by combining rate and mass differences. For concreteness, we will focus on the comparison between supersymmetry and the same-spin scenario defined in equation (1). We will assume the final decay products always include stable neutral particles. Of course, this would be the lightest supersymmetric particle (LSP) in the case of SUSY. We will assume the existence of such a stable particle, denoted by A, in the case of same-spin scenario due to the implementation of certain discrete symmetry. Examples which have qualitatively the same feature as such

a scenario include Universal Extra-Dimensions [27] and little Higgs models with *T*-parity [28, 29].

For simplicity, we will only consider simple decay chains following the production. A study of a set of models with more complicated decay chains is beyond the scope of this initial paper. We will briefly comment on such scenarios in the conclusion.

4.1. Degeneracy with rate and mass differences

As pointed out in [38] and [6], typical transverse variables are largely sensitive to the mass differences between the initial and subsequent particles in the decay chain. This is also a physics reason for the set of degeneracies in measuring mass parameters within supersymmetry, pointed out in [39]. Therefore, in a particular channel, there can be a degeneracy between supersymmetry and an alternative scenario with the same-spin partners. Schematically, suppose the production cross section for some superpartner of mass m is σ_m^{SUSY}. We could choose the mass of a similar partner in the alternative scenario, m', so that the production cross section matches, $\sigma_{m'}^{\text{altn}} = \sigma_m^{\text{SUSY}}$. At the same time, we could learn from some transverse kinematical variables the information about mass differences in supersymmetry, say $\Delta m = m - m_{\text{LSP}}$. However, if those variables mainly contain information about mass differences (which is true to a pretty good approximation), we can adjust the mass difference in the alternative scenario, $\Delta m' = m' - m_A$, to fix the kinematical distribution as well. If other information is available about the mass, that can remove the degeneracy, but typically that will not occur with early collider data.

We demonstrate this degeneracy in a simple example. Consider the comparison between a squark and some fermionic quark partner q'. Let's also assume they are both pair produced, and followed by similar simple decay chains $\tilde{q} \rightarrow q + \text{LSP}$ and $q' \rightarrow q + A$, where A is some stable neutral particle, analogous to the LSP in SUSY models. In our simulation, we generate parton-level events with MadGraph/MadEvent [40] for the squark pair production and decay $pp \rightarrow \tilde{q}\tilde{q}^* \rightarrow q\bar{q} + 2\,\text{LSP}$, as well as the q' pair production and decay $pp \rightarrow q'q'^* \rightarrow q\bar{q}AA$.[7] Then the parton-level events are passed to PYTHIA 6.4 [42] for parton shower, fragmentation and PGS4 [43] for detector reconstruction. It is straightforward to match the production rate by choosing appropriate $m_{\tilde{q}}$ and $m_{q'}$. For example, $m_{\tilde{q}} = 549$ GeV and $m_{q'} = 900$ GeV both give rise to $\sigma \approx 2$ pb. In the above examples, we have not decoupled the color octet particles, but this will not affect our discussion below.

Next, we adjust the mass of the missing particle to match the kinematical distributions. Note that choosing the mass difference to be the same, $\Delta m = m_{\tilde{q}} - m_{\text{LSP}} = m_{q'} - m_A$, will give rise to significant difference in kinematical distribution, particularly when the mass difference is large. Indeed, in order to match the rate, we have to choose $m_{q'}$ to be significantly greater than $m_{\tilde{q}}$. Therefore, choosing a large and fixed mass difference usually implies $\Delta m \gg m_{\text{LSP}}$. In this case, the available energy $\sim \Delta m$ tends to be shared evenly between the LSP and the rest of the observable decay products (q in this case). On the other hand, in the alternative scenario, we usually have Δm much closer to the missing particle mass m_A. It is therefore typical for the recoiling quark to have a harder spectrum. In the figure 4, we plot the H_T[8] distribution for $\tilde{q}$ and q' pair productions. In both cases, we keep the same mass difference $\Delta m = 452$ GeV, i.e. $m_{\text{LSP}} = 97$ GeV and $m_A = 448$ GeV. One can check that the difference in the average of the H_T does match correctly with the theoretical expectation.

---

[7] Here, for simplicity, we have not included the $\tilde{q}\tilde{q}$ and $q'q'$ final states, and only included the quark partners of u_R in the final state.

[8] Effective mass is defined as $H_T = \not{E}_T + \sum_{\text{all jets}} P_T^a$
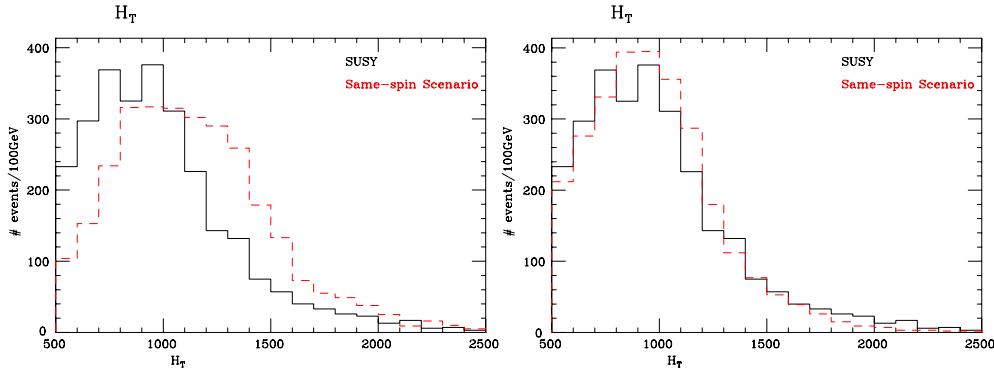
Figure 4. Left: H_T distributions for squark pair production (solid line) and q' pair production (dashed line) at LHC with both the cross section and mass difference matched. The mass parameters involved are $m_{\tilde{q}} = 549$ GeV, $m_{q'} = 900$ GeV, $m_{LSP} = 97$ GeV and $m_A = 448$ GeV. Right: H_T distributions for the same processes but with the mass difference adjusted in the same-spin scenario. The mass of the missing particle now is $m_A = 548$ GeV. In both cases, we have generated 3000 events, corresponding to approximately 1.5 fb^{-1} integrated luminosity.

However, this does not imply the absence of the degeneracy. The key requirement for the existence of such a degeneracy is that the transverse variables are approximately functions of *only* mass differences, even if the functions may be different for different scenarios. In this case, it is still possible to adjust the mass difference in both scenarios to obtain indistinguishable distributions, even though the mass differences will be different in those cases. Although this requires very specific masses, it is important that we address this possibility in order to have a robust spin determination method. We can see this again in the example of squark production and decay. For the examples we just considered, if M_A is increased to 548 GeV, then one cannot distinguish the H_T of these two cases as seen in the figure 4.

A similar conclusion applies to three body decays such as $\tilde{g} \rightarrow q\bar{q} + $LSP. More explicitly, we consider supersymmetric and same-spin partners, which have about the same production rate ($\sigma \approx 0.8$ pb) and mass splitting:

- $m_{\tilde{g}} = 800$ GeV, $m_{LSP} = 137$ GeV
- $m_{g'} = 1060$ GeV, $m_A = 397$ GeV.

The H_T distributions for both productions are plotted in figure 5. Again we can adjust the mass difference in the same-spin scenario such that the two distributions match. This can be seen in figure 5, where we have increased m_A to 497 GeV.

Before proceeding further, we remark that there is a possibility that we could tell that the partners are from the same-spin scenario and not supersymmetry. Assume the new physics discovered at the LHC is actually in the same-spin scenario. We want to verify whether a supersymmetric scenario could match the rate and the same kinematical distributions. Because of the difference in production rate, the supersymmetric scenario will necessarily have a much lighter colored partner, squark or gluino, or both. Then, in order to macth the H_T distribution, we must have at least comparable mass gaps between the colored partner and the missing particle. Therefore, there is a possibility in this case that we cannot find a solution for the supersymmetric scenario. For example, from the previous discussion, we know that, to match a cross section about 0.8 pb, either a gluino with mass $m_{\tilde{g}} = 800$ GeV or a g' with mass $m_{g'} = 1060$ GeV is required. However, if the mass difference is measured to be larger than 700 GeV, then the supersymmetric scenario is excluded since otherwise the LSP mass is below the LEP II bound.
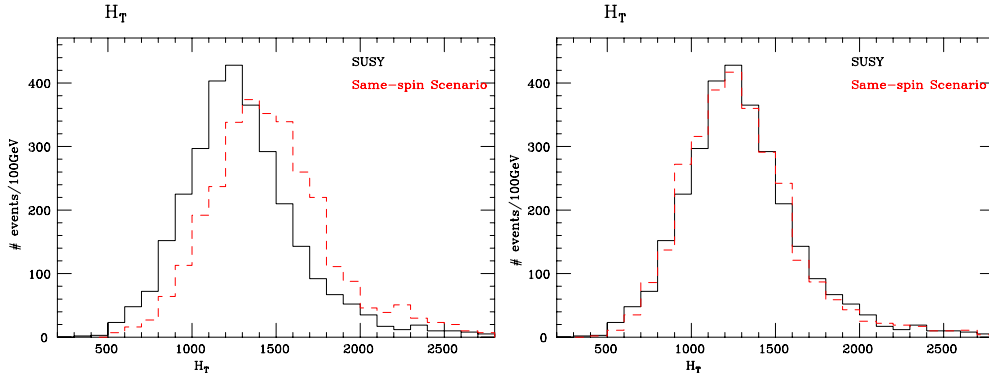
8

Figure 5. Left: H_T distributions for gluino pair production (solid line) and g' pair production (dashed line) at LHC with both the cross section and the mass difference matched. The mass parameters involved are $m_{\tilde{g}} = 800$ GeV, $m_{q'} = 1060$ GeV, $m_{\text{LSP}} = 137$ GeV and $m_A = 397$ GeV. Right: H_T distributions for the same processes but with the mass difference adjusted in the same-spin scenario. The mass of the missing particle is now $m_A = 497$ GeV. In both cases, we have generated 3000 events, corresponding to approximately 3.75 fb^{-1} integrated luminosity.

4.2. Matching multichannels

As we have seen so far, there are purely kinematical differences for models with different mass of the decaying particle. We also note that these differences are generally not very significant for measuring spins since the mass difference Δm can be adjusted independently of the mass of the decaying particle. A more detailed analysis for these situations is certainly necessary to explore such differences for spin determination. However, in reality, there will be more handles to distinguish spin using the rate information. A complete model usually contains several other new particles beside the color octet. In many theories, we expect the masses of the colored partners to be similar, i.e. around TeV scale. Therefore, at least several of them will be copiously produced at the LHC. We should consider the production channels of those colored states together. We will then have more observables which we could use to break the degeneracy discussed above. In this section, we present a method to achieve this goal by combining information from several channels. We show that this method, based on a set of simple observables, is effective and independent of mass measurement.

To demonstrate our method, we focus on distinguishing supersymmetry and the same-spin scenario. We start with the case in which the squark mass is lighter than the gluino mass, so gluinos decay through a two-body process. In our example, the gluino and squark masses are taken to be $m_{\tilde{g}} = 608$ GeV and $m_{\tilde{q}} = 549$ GeV. Then we find that to match the gluino pair production rate, the g' mass is fixed to be $m_{g'} = 850$ GeV. Furthermore we match the gluino–squark production rate by varying the q' mass, which leads to $m_{q'} = 790$ GeV. This can be seen from figure 6, where the two vertical dashed lines correspond to the masses of $\tilde{g}$ and q' while the horizontal dashed line corresponds to 20 pb for the cross section of the associated production. After this matching, the cross sections of $\tilde{q}\tilde{q}$ and $q'q'$ productions are fixed to be about 8 pb and 19 pb, respectively. The cross sections for both models are calculated in MadGraph/MadEvent and are:

$$\text{SUSY}: \quad \sigma_{\tilde{g}\tilde{g}} \approx 4\,\text{pb}, \qquad \sigma_{\tilde{g}\tilde{q}} \approx 20\,\text{pb}, \qquad \sigma_{\tilde{q}\tilde{q}} \approx 8\,\text{pb}$$

$$\text{Same-Spin Scenario}: \quad \sigma_{g'g'} \approx 4\,\text{pb}, \qquad \sigma_{g'q'} \approx 20\,\text{pb}, \qquad \sigma_{q'q'} \approx 19\,\text{pb}. \tag{5}$$
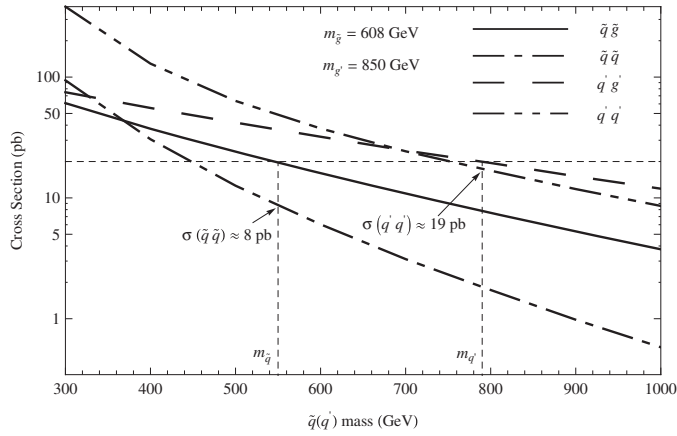
9

Figure 6. Production cross sections for $\tilde{g}\tilde{q}$ production (solid line), $g'q'$ pair production (dashed line), $\tilde{q}\tilde{q}$ production (dash-dot line) and $q'q'$ production (dash-dot-dot line). The $\tilde{g}\tilde{g}$ and $g'g'$ production cross sections are already matched by choosing gluino mass $m_{\tilde{g}} = 608$ GeV and g' mass $m_{g'} = 850$ GeV. The horizontal dashed line corresponds to 20 pb for the cross section of the associated production. If we match to this rate, the squark mass is 549 GeV and the q' mass is 790 GeV as indicated by the vertical dashed lines. After this matching, the cross section of $\tilde{q}\tilde{q}$ and $q'q'$ productions are fixed to be about 8 pb and 19 pb, respectively.

One can see that the rate of q' pair production cannot be matched with that of the squark pair production at the same time as other rates are matched.

More generally, we note that the cross section of gluino (g') pair production is almost independent of the squark (q') mass. Therefore, by matching the cross sections for gluino and g' pair production, the g' mass is fixed for a given gluino mass. After that, the gluino–squark (g'–q') cross section only changes as squark (q') mass varies. Figure 6 shows a plot displaying the cross sections as functions of squark (q') mass with gluino (g') mass fixed. As we can see from this figure, generally, the three production rates cannot be matched at the same time. In addition, such matching will typically force us to consider quite different mass splittings. Therefore, we also expect the typical jet transverse momentum variable, such as H_T, will be quite different.

The discussions above on matching individual cross sections are obviously a simplification to demonstrate the principles. In reality, after showering and forming the jets, the channels considered above can give sizable overlapping contributions to the same final state. Therefore, instead of matching the cross section for each channel, we perform next a more realistic study by matching directly to observables, in particular, the jet multiplicity and p_T distribution (again using H_T as a representative example). Generally, we expect no degeneracy even by considering the jet multiplicities. The reason is as follows. Since we are including another particle in the analysis, there are three mass variables in the models. These three variables can be fixed by matching the total cross section and the two H_T peaks (if the masses of the two color particles are considerably different). Because of the difference in the spins in the two models, the ratios of the cross sections between different channels are generically different. Therefore, the jet counts are not likely to be the same, because these channels have different jet multiplicities.

4.2.1. Case I: $m_{\tilde{g}} > m_{\tilde{q}}$. Let us start with the case where the gluino is heavier than the squark in the SUSY model. For simplicity, we take it to be the SUSY model with mass parameters

Table 1. This table shows $(\overline{H}_T, \Delta S)$ for each same-spin model parameterized by three mass parameters $m_{g'}$, $m_{q'}$ and m_A for Case I. Here ΔS is defined in equation (6). In each column, a set of $(m_{g'}, m_{q'})$ is chosen to match the total cross section with that of the SUSY model, which is defined by $m_{\tilde{g}} = 608$ GeV, $m_{\tilde{q}} = 549$ GeV and $m_{\text{LSP}} = 97$ GeV. In each row, a mass m_A is specified, which can be seen from the first column. For the SUSY model in the comparison, $\overline{H}_T = 913$ GeV, and the jet counts are given by {189, 965, 620, 171, 46} for jet number $n_j = 1, 2, 3, 4, 5+$. The data indicate that H_T and jet multiplicity of the same-spin model cannot be matched to those in the SUSY model simultaneously.

m_A (GeV)	Same Spin Models $(m_{g'}, m_{q'})$ (GeV)					
	(1000, 640)	(950, 720)	(900, 800)	(850, 880)	(800, 960)	(750, 1120)
100	(1218, 6.6)	(1271, 7.9)	(1307, 7.2)	(1373, 7.7)	(1399, 13.4)	(1474, 16.4)
250	(1104, 5.8)	(1178, 6.4)	(1218, 6.2)	(1254, 8.0)	(1289, 16.8)	(1339, 20.0)
400	(875, 3.2)	(984, 5.1)	(1036, 4.8)	(1057, 7.2)	(1072, 17.2)	(1103, 18.4)
550	(584, 6.5)	(682, 2.7)	(767, 2.5)	(776, 3.9)	(758, 14.6)	(820, 12.0)
700	–	(452, 18.7)	(427, 6.0)	(410, 7.4)	(456, 6.4)	(706, 14.2)

$m_{\tilde{g}} = 608$ GeV, $m_{\tilde{q}} = 549$ GeV and $m_{\text{LSP}} = 97$ GeV. The total cross section of the $\tilde{g}\tilde{g}$, $\tilde{q}\tilde{q}$ and $\tilde{g}\tilde{q}$ final states is approximately 31.6 pb. Then by varying the mass parameters $m_{g'}$ and $m_{q'}$ in the same-spin scenario, one can match the total rate of the SUSY model; several choices of masses are listed in table 1. For each of these models, we generate 2000 events in MadEvent–BRIDGE–Pythia–PGS setup[9] and compare the jet multiplicities with those of the SUSY model. The decay of the gluino is a two-body process $\tilde{g} \to \tilde{q} + q$, followed by the decay of squark $\tilde{q} \to q + \text{LSP}$. Here we include the first two generations of squarks for simplicity[10]. For the same-spin scenario, we consider the similar decay processes of g' and q': $g' \to q' + q$ and $q' \to q + A$. Once the jet counts are obtained, the difference between SUSY and same-spin scenario can be characterized by defining a χ-square-like quantity

$$(\Delta S)^2 = \frac{1}{N} \sum_{i=1}^{N} \left(\frac{n_i^{\text{SUSY}} - n_i^{\text{SameSpin}}}{\sigma_i} \right)^2. \tag{6}$$

In the following, we consider jet counts for $N = 5$ bins with $n_{\text{jet}} = 1, 2, 3, 4, 5+$. Here n_i^{SUSY} $\left(n_i^{\text{SameSpin}} \right)$ is the number of events in each bin for the SUSY (same spin) model. The standard deviation is defined by $\sigma_i^2 \equiv \left(\sigma_i^{\text{SameSpin}} \right)^2 + \left(\sigma_i^{\text{SUSY}} \right)^2$, where $\sigma_i = \sqrt{n_i + 1}$ for each model. In our simulation, we have used the PGS4 default detector configuration and cone jet algorithm with a cone size 0.5. In addition, we use the PGS trigger with low thresholds:

- Inclusive $\not{E}_T$ 90 GeV
- Inclusive single-jet 400 GeV
- Jet plus $\not{E}_T$ (180 GeV, 80 GeV)
- Accoplanar jet and $\not{E}_T$ (100 GeV, 80 GeV, $1 < \Delta\phi < 2$)
- Accoplanar dijets (200 GeV, $\Delta\phi < 2$).

To be realistic, we also impose the selection cuts for jets: $P_T \geqslant 50$ GeV and $\eta < 2.5$.

In table 1, the average of H_T and the value of ΔS are shown for given $m_{g'}$, $m_{q'}$ and m_A. For the SUSY model in the comparison, the average of H_T is 913 GeV, and the jet counts are {189, 965, 620, 171, 46} for jet number $n_j = 1, 2, 3, 4, 5+$. As can be seen from the table, values of ΔS are generically large for cases with $m_{q'} > m_{g'}$. This can be understood since in

---

[9] We use BRIDGE [44] to decay the parton events containing the gluino (g') and squark (q') before Pythia and PGS.
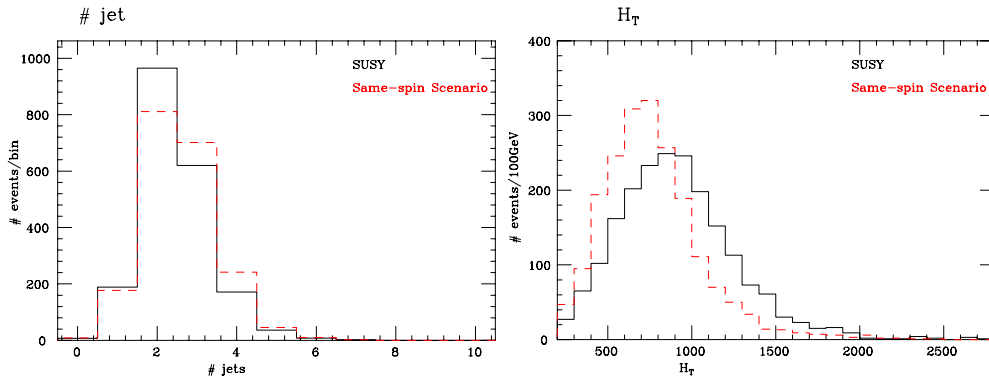[10] The third generation squarks (q') will decay into b-jets which can be tagged and studied separately.

Figure 7. Left: the jet counts for the SUSY model (solid line) in the Case I and the same-spin model (dashed line) which has the smallest ΔS in table 1. We vary mass parameters $m_{\tilde{g}}$, $m_{\tilde{q}}$ and m_{LSP} for the SUSY model, and $m_{g'}$, $m_{q'}$ and m_A for the same-spin model. Both models are tuned to have the same total cross section. Right: the H_T distributions for the same pair of models: the SUSY model (solid line) and the same-spin model (dashed line). Both plots contain 2000 events, corresponding to approximately 70 pb^{-1} integrated luminosity.

this case q' and g' decay very differently from squark and gluino. However, for cases with $m_{q'} < m_{g'}$, ΔS can be smaller. The same-spin model with the smallest ΔS in the table is the one with $m_{g'} = 900$ GeV, $m_{q'} = 800$ GeV and $m_A = 550$ GeV, where $\Delta S = 2.5$. The jet multiplicity and H_T distribution are shown in figure 7. First of all, one can see that ΔS is not small, and so the jet multiplicity is not completely matched[11]. Second, even if ΔS is small, the H_T distribution is different enough to eliminate the possible degeneracy. So based on the above observations, one can see that the degeneracy is unlikely to exist considering total cross section, H_T and jet multiplicity simultaneously.

4.2.2. Case II: $m_{\tilde{g}} < m_{\tilde{q}}$. For the case where the squark is heavier than the gluino in the SUSY model, we consider the following example: $m_{\tilde{g}} = 640$ GeV, $m_{\tilde{q}} = 800$ GeV and $m_{\text{LSP}} = 100$ GeV. The total cross section of the $\tilde{g}\tilde{g}$, $\tilde{q}\tilde{q}$ and $\tilde{g}\tilde{q}$ final states is approximately 11.3 pb. In such a case, the jet multiplicity can be matched better for same-spin models with q' heavier than g'. First we vary the masses of g' and q' to match the total cross section, where four possible choices of $(m_{g'}, m_{q'})$ are listed in table 2.[12] The decay processes are simplified by taking $\tilde{q} \rightarrow \tilde{g} + q$ and $\tilde{q} \rightarrow q + \bar{q} + \text{LSP}$, and similarly for q' and g'. As seen from the table, the best fit of jet multiplicity is achieved when $m_{g'} = 950$ GeV, $m_{q'} = 1120$ GeV and $m_A = 600$ GeV, where $\Delta S = 0.8$. The jet multiplicity and H_T distribution are shown in figure 8. Though the jet multiplicities are well matched, the differences (both the width and the position of the peak) in the H_T distributions should be enough to distinguish them. Therefore, again we see that matching the H_T distributions and matching the jet multiplicities are in conflict with each other and cannot be satisfied simultaneously. As long as squarks are not too heavy and the production rate is of about the same order of magnitude as that of gluino, the above considerations are reasonable. The analysis may be difficult when squarks become much heavier than gluinos.

---

[11] It actually cannot be further reduced by tuning the mass parameters.
[12] The reason to choose these four cases is that $m_{q'} - m_{g'}$ is close to $m_{\tilde{q}} - m_{\tilde{g}}$. For large mass difference, it should have larger kinematical difference.
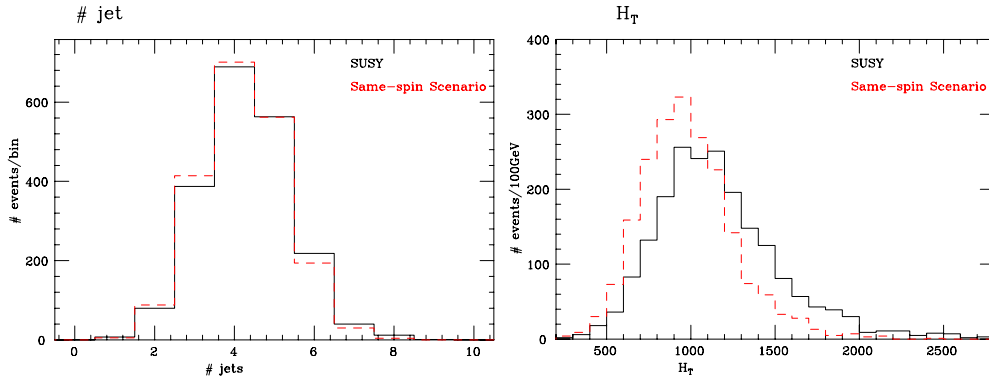
Figure 8. Left: the jet counts for the SUSY model (solid line) in the Case II and the same-spin model (dashed line) which has the smallest ΔS in table 2. We vary mass parameters $m_{\tilde{g}}$, $m_{\tilde{q}}$ and m_{LSP} for the SUSY model, and $m_{g'}$, $m_{q'}$ and m_A for the same-spin model. Both models are tuned to have the same total cross section. Right: the H_T distributions for the same pair of models: the SUSY model (solid line) and the same-spin model (dashed line). Both plots contain 2000 events, corresponding to approximately 200 pb^{-1} integrated luminosity.

Table 2. This table shows $(\overline{H}_T, \Delta S)$ for each same-spin model parameterized by three mass parameters $m_{g'}$, $m_{q'}$ and m_A for Case II. Here ΔS is defined in equation (6). In each column, a set of $(m_{g'}, m_{q'})$ is chosen to match the total cross section with that of the SUSY model, which is defined by $m_{\tilde{g}} = 640$ GeV, $m_{\tilde{q}} = 800$ GeV and $m_{\mathrm{LSP}} = 100$ GeV. In each row, a mass m_A is specified, which can be seen from the first column. For the SUSY model in the comparison, $\overline{H}_T = 1161$ GeV, and the jet counts are given by {7, 80, 387, 689, 834} for jet number $n_j = 1, 2, 3, 4, 5+$. The data indicate that H_T and jet multiplicity of the same-spin model cannot be matched to those in the SUSY model simultaneously.

m_A (GeV)	Same Spin Models $(m_{g'}, m_{q'})$ (GeV)			
	(1000, 1020)	(950, 1120)	(900, 1240)	(850, 1400)
100	(1530, 9.6)	(1657, 5.6)	(1713, 7.2)	(1692, 5.8)
200	(1478, 8.9)	(1585, 5.5)	(1643, 7.0)	(1639, 6.1)
400	(1258, 10.3)	(1358, 4.3)	(1377, 4.6)	(1381, 2.6)
600	(914, 13.6)	(984, 0.8)	(1015, 2.8)	(1037, 5.6)
800	(474, 20.4)	(560, 15.3)	(701, 19.8)	(961, 22.5)

So far we have demonstrated that there is finally no degeneracy for the cases we studied. However, for realistic models, both the squarks (q') and gluinos (g') could decay through many different channels, leading to longer decay chain and more final-state particles. This could change the jet multiplicity and jet P_T significantly, and it is not clear whether there are degeneracies or not in these situations. If there were, one would expect including more observables would again eliminate the degeneracy. On the other hand, when LHC data are available, one may be able to learn something about the decay topology or decay branching ratios. Given that information, the potential model dependence can be reduced. Finally, if there is no degeneracy, then one can figure out the spin of gluino or squark by fitting to the data.

5. Conclusions

We present a new method of determining the spins of TeV scale new physics particles by utilizing production rate information. Basically, if the mass and the production cross section

are measured, the spin is then determined. For many forms of new physics that might be discovered, the method will work well. Degeneracies may occur, in which case further analysis is needed, which is provided. After clarifying the degeneracy in spin measurement by using rate information in a single production channel, we propose to combine information, such as jet counts and H_T distributions, from several channels. This method will be particularly useful for an early determination of spin of the colored new physics particles since we expect at least several of them will be produced copiously. Such a method does not require precise mass measurement. In particular, we consider two cases where the SUSY models are characteristically different: $m_{\tilde{g}} > m_{\tilde{q}}$ and $m_{\tilde{g}} < m_{\tilde{q}}$. For the first case with a specific set of SUSY mass parameters ($m_{\tilde{g}}$, $m_{\tilde{q}}$ and m_{LSP}), we find that the jet multiplicity cannot be well matched by the same-spin model with similar mass parameters ($m_{g'}$, $m_{q'}$ and m_A). In addition, the H_T distribution shows extra difference from that of the SUSY model. For the second case, we find that the jet multiplicity can be well matched by the same-spin model. However, the difference in the H_T distribution can be used to distinguish these two scenarios. The reason why this method works relies on the fact that the production cross sections encode the spin information of the SM partners in a nontrivial way, which lead to signals which can be used to distinguish scenarios with different spin assignments. In some cases, the pure rate signal may be hard to see due to special mass splittings. However, the kinematical differences are generically present and allow us to distinguish these scenarios eventually.

Detailed study of spin determination using our method is certainly needed. First of all, although we have imposed certain selection cuts which mimic those would be used in Standard Model background suppression, a precise evaluation of the effectiveness of our method can only be obtained after carefully including full background and more realistic detector effects.

We have demonstrated our method using simple decay chains, which could be the dominant ones in realistic models. At the same time, more complicated decay patterns could well occur. On the one hand, such decay channels, especially those with leptons, will greatly enhance the discovery potential and signal-to-background ratio, which could improve the sensitivity of method. On the other hand, they could introduce more model dependence. A detailed study of disentangling of those effects is certainly important and useful, which will be discussed in follow-up papers.

References

[1] Barr A J 2004 *Phys. Lett.* B **596** 205 (arXiv:hep-ph/0405052)
[2] Smillie J M and Webber B R 2005 *J. High Energy Phys.* JHEP10(2005)069 (arXiv:hep-ph/0507170)
[3] Wang L T and Yavin I 2007 *J. High Energy Phys.* JHEP04(2007)032 (arXiv:hep-ph/0605296)
[4] Smillie J M 2007 *Eur. Phys. J.* C **51** 933 (arXiv:hep-ph/0609296)
[5] Csaki C, Heinonen J and Perelstein M 2007 *J. High Energy Phys.* JHEP10(2007)107 (arXiv:0707.0014 [hep-ph])
[6] Meade P and Reece M 2006 *Phys. Rev.* D **74** 015010 (arXiv:hep-ph/0601124)
[7] Alves A, Eboli O and Plehn T 2006 *Phys. Rev.* D **74** 095010 (arXiv:hep-ph/0605067)
[8] Bachacou H, Hinchliffe I and Paige F E 2000 *Phys. Rev.* D **62** 015009 (arXiv:hep-ph/9907518)
[9] Allanach B C, Lester C G, Parker M A and Webber B R 2000 *J. High Energy Phys.* JHEP09(2000)004 (arXiv:hep-ph/0007009)
[10] Gjelsten B K, Miller D J and Osland P 2004 *J. High Energy Phys.* JHEP12(2004)003 (arXiv:hep-ph/0410303)
[11] Gjelsten B K, Miller D J and Osland P 2005 *J. High Energy Phys.* JHEP06(2005)015 (arXiv:hep-ph/0501033)
[12] Lester C G 2007 *Phys. Lett.* B **655** 39 (arXiv:hep-ph/0603171)
[13] Lester C G, Parker M A and White M J 2006 *J. High Energy Phys.* JHEP01(2006)080 (arXiv:hep-ph/0508143)
[14] Ross G G and Serna M 2007 arXiv:0712.0943 (hep-ph)
[15] Barr A J, Gripaios B and Lester C G 2007 arXiv:0711.4008 [hep-ph]
[16] Cho W S, Choi K, Kim Y G and Park C B 2007 arXiv:0711.4526 [hep-ph]
[17] Lester C and Barr A 2007 arXiv:0708.1028 [hep-ph]
[18] Cheng H C, Gunion J F, Han Z, Marandella G and McElrath B 2007 arXiv:0707.0030 [hep-ph]
[19] Cheng H C, Engelhardt D, Gunion J F, Han Z and McElrath B 2008 arXiv:0802.4290 [hep-ph]
[20] Tovey D R 2001 *Phys. Lett.* B **498** 1 (arXiv:hep-ph/0006276)
[21] Hinchliffe I, Paige F E, Shapiro M D, Soderqvist J and Yao W 1997 *Phys. Rev.* D **55** 5520 (arXiv:hep-ph/9610544)
[22] The CDF Collaboration *Conf. Note 8148* http://www-cdf.fnal.gov/physics/new/top/public_xsection.html
[23] The D0 Collaboration *D0 Note 5591-CONF* http://www-d0.fnal.gov/Run2Physics/WWW/results/prelim/TOP/T64/
[24] The CDF Collaboration *Conf. Note 9214* http://www-cdf.fnal.gov/physics/new/top/public_mass.html
[25] The D0 Collaboration *D0 Note 5498-CONF* http://www-d0.fnal.gov/Run2Physics/WWW/results/prelim/TOP/T63/
[26] Datta A, Kane G L and Toharia M 2005 arXiv:hep-ph/0510204
[27] Appelquist T, Cheng H C and Dobrescu B A 2001 *Phys. Rev.* D **64** 035002 (arXiv:hep-ph/0012100)
[28] Cheng H C and Low I 2003 *J. High Energy Phys.* JHEP09(2003)051 (arXiv:hep-ph/0308199)
[29] Cheng H C and Low I 2004 *J. High Energy Phys.* JHEP08(2004)061 (arXiv:hep-ph/0405243)
[30] Beenakker W, Hopker R, Spira M and Zerwas P M 1997 *Nucl. Phys.* B **492** 51 (arXiv:hep-ph/9610490)
[31] Plehn T, Rainwater D and Skands P 2007 *Phys. Lett.* B **645** 217 (arXiv:hep-ph/0510144)
[32] Beenakker W, Kramer M, Plehn T, Spira M and Zerwas P M 1998 *Nucl. Phys.* B **515** 3 (arXiv:hep-ph/9710451)
[33] Bityukov S I and Krasnikov N V 1997 *Mod. Phys. Lett.* A **12** 2011 (arXiv:hep-ph/9705338)
     Manohar A V and Wise M B 2006 *Phys. Rev.* D **74** 035009 (arXiv:hep-ph/0606172)
     Gresham M I and Wise M B 2007 *Phys. Rev.* D **76** 075003 (arXiv:0706.0909 [hep-ph])
[34] Macesanu C, McMullen C D and Nandi S 2002 *Phys. Rev.* D **66** 015009 (arXiv:hep-ph/0201300)
[35] Dawson S, Eichten E and Quigg C 1985 *Phys. Rev.* D **31** 1581
[36] Beenakker W, Hopker R, Spira M and Zerwas P M 1997 *Nucl. Phys.* B **492** 51 (arXiv:hep-ph/9610490)
[37] Yao W M *et al* (Particle Data Group) 2006 *J. Phys. G: Nucl. Part. Phys.* **33** 1
[38] Cheng H C, Low I and Wang L T 2006 *Phys. Rev.* D **74** 055001 (arXiv:hep-ph/0510225)
[39] Arkani-Hamed N, Kane G L, Thaler J and Wang L T 2006 *J. High Energy Phys.* JHEP08(2006)070 (arXiv:hep-ph/0512190)
[40] Maltoni F and Stelzer T 2003 *J. High Energy Phys.* JHEP02(2003)027 (arXiv:hep-ph/0208156)
     Alwall J *et al* 2007 *J. High Energy Phys.* JHEP09(2007)028 (arXiv:0706.2334 [hep-ph])
[41] Pumplin J, Stump D R, Huston J, Lai H L, Nadolsky P and Tung W K 2002 *J. High Energy Phys.* JHEP07(2002)012 (arXiv:hep-ph/0201195)
[42] Sjostrand T, Mrenna S and Skands P 2006 *J. High Energy Phys.* JHEP05(2006)026 (arXiv:hep-ph/0603175)
[43] http://www.physics.ucdavis.edu/conway/research/software/pgs/pgs4-general.htm
[44] Meade P and Reece M 2007 arXiv:hep-ph/0703031